

# Water-Enhanced Direct Air Capture of Carbon Dioxide in Metal–Organic Frameworks

Oscar Iu-Fan Chen, Cheng-Hsin Liu, Kaiyu Wang, Emilio Borrego-Marin, Haozhe Li, Ali H. Alawadhi, Jorge A. R. Navarro,\* and Omar M. Yaghi\*



Cite This: *J. Am. Chem. Soc.* 2024, 146, 2835–2844



Read Online

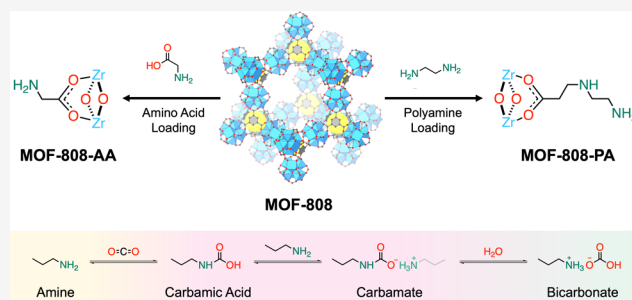
ACCESS |

Metrics & More

Article Recommendations

Supporting Information

**ABSTRACT:** We have developed two series of amine-functionalized zirconium (Zr) metal–organic framework-808 (MOF-808), which were produced by postsynthetic modifications to have either amino acids coordinated to Zr ions (MOF-808-AAs) or polyamines covalently bound to the chloro-functionalized structure (MOF-808-PAs). These MOF variants were comprehensively characterized by liquid-state  $^1\text{H}$  nuclear magnetic resonance (NMR) measurements and potentiometric acid–base titration to determine the amounts of amines, energy-dispersive X-ray spectroscopy to assess the extent of covalent substitution by polyamines, powder X-ray diffraction analysis to verify the maintenance of the MOF crystallinity and structure after postsynthetic modifications, nitrogen sorption isotherm measurements to confirm retention of the porosity, and water sorption isotherm measurements to find the water uptake in the pores of each member of the series. Evaluation and testing of these compounds in direct air capture (DAC) of  $\text{CO}_2$  showed improved  $\text{CO}_2$  capture performance for the functionalized forms, especially under humid conditions: In dry conditions, the L-lysine- and tris(3-aminopropyl)amine-functionalized variants, termed as MOF-808-Lys and MOF-808-TAPA, exhibited the highest  $\text{CO}_2$  uptakes at 400 ppm, measuring 0.612 and 0.498  $\text{mmol g}^{-1}$ , and further capacity enhancement was achieved by introducing 50% relative humidity, resulting in remarkable uptakes of 1.205 and 0.872  $\text{mmol g}^{-1}$  corresponding to 97 and 75% increase compared to the dry uptakes, respectively. The mechanism underlying the enhanced uptake efficiency was revealed by  $^{13}\text{C}$  solid-state NMR and temperature-programmed desorption measurements, indicating the formation of bicarbonate species, and therefore a stoichiometry of 1:1  $\text{CO}_2$  to each amine site.



## INTRODUCTION

The fast-paced development of industry and technology has led to a significant increase in energy demands, heavily reliant on the combustion of fossil fuels, which has resulted in the emission of substantial amounts of carbon dioxide ( $\text{CO}_2$ ), contributing to severe environmental issues.<sup>1</sup> In light of this, a crucial solution to combat  $\text{CO}_2$  emissions from the atmosphere is through the implementation of direct air capture (DAC).<sup>2–4</sup> To effectively capture  $\text{CO}_2$  from the ambient air, which is present at a low concentration (0.04%), it is essential to have highly reactive specific sites for  $\text{CO}_2$  adsorption. In this context, amine functionalities have emerged as promising candidates for chemisorption sites, facilitating the development of efficient  $\text{CO}_2$  capture sorbents.<sup>5–11</sup> While current methods involve using aqueous alkaline solutions<sup>12,13</sup> to chemically bind  $\text{CO}_2$ , they suffer from significant drawbacks such as energy-intensive desorption processes and poor long-term cyclability. These issues result in high energy consumption and unavoidable secondary  $\text{CO}_2$  emissions, leading to elevated costs. Therefore, it is imperative to develop new materials to study and address these challenges.

Numerous categories of solid-state materials have undergone extensive exploration to fulfill the criteria for efficient  $\text{CO}_2$  sorbents and to decipher the  $\text{CO}_2$  sorption chemistry, including zeolites,<sup>5,14</sup> polymers,<sup>8,15,16</sup> silicas,<sup>10,17–19</sup> metal–organic frameworks (MOFs),<sup>7,20–26</sup> and covalent organic frameworks (COFs).<sup>9,27</sup> In our prior research endeavors,<sup>28</sup> we formulated and synthesized a sequence of coordinatively amino acid-functionalized MOF-808 materials, termed MOF-808-AAs (AA = amino acid anion), with the primary aim of elucidating the mechanism underlying  $\text{CO}_2$  capture via amine moieties. We thus observed the favorable amine– $\text{CO}_2$  interaction attributed to the generation of bicarbonate species<sup>28,29</sup> facilitated by water vapor. Expanding upon this foundational understanding, our current investigations have led us to develop a new series of postsynthetically functionalized

**Received:** December 13, 2023

**Revised:** December 31, 2023

**Accepted:** January 5, 2024

**Published:** January 18, 2024



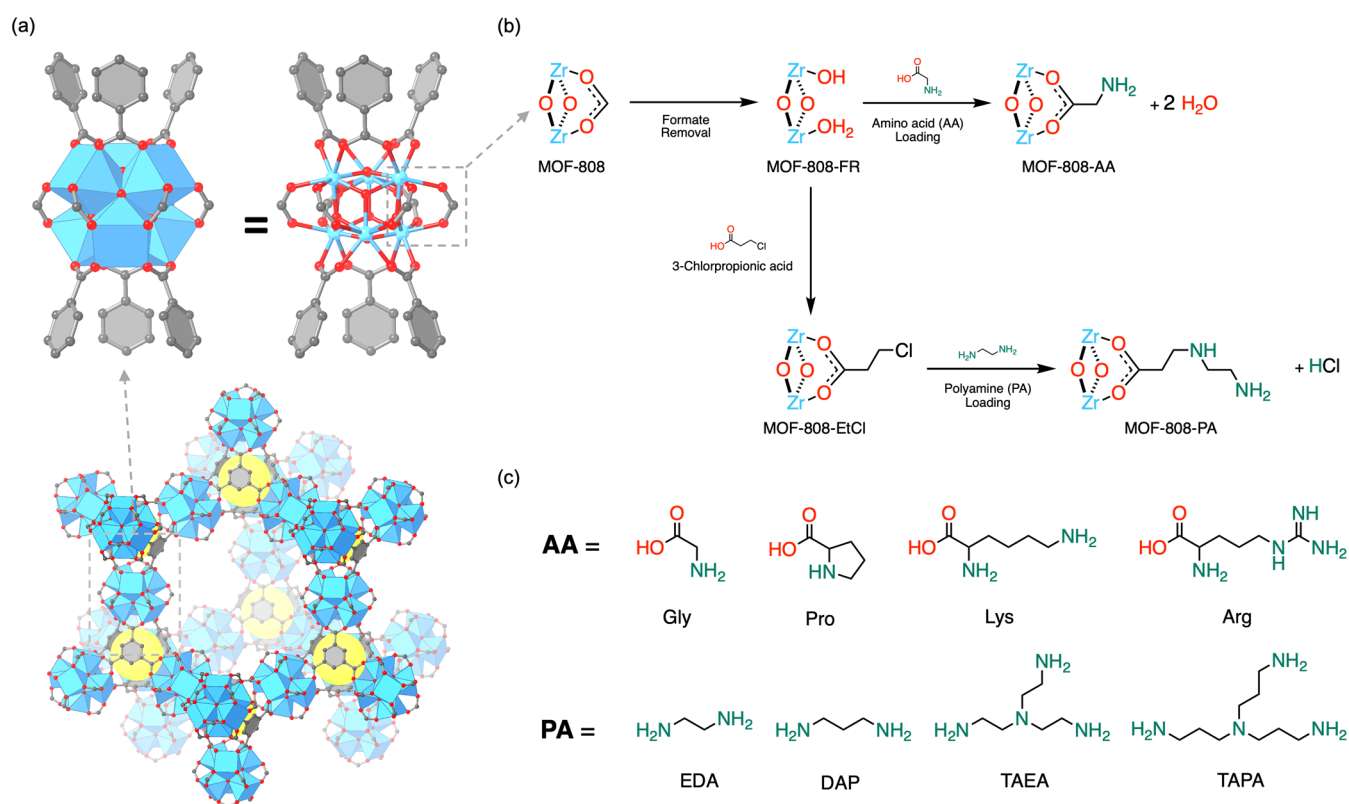


**Figure 1.** (a) Structure of MOF-808 and (b) general synthetic scheme for MOF-808-AA and MOF-808-PA. (c) Selected installed amino acids and polyamines. Zr atoms are represented as light blue polyhedra or spheres, while other atoms are represented as spheres (color code: C, gray; and O, red). H atoms are omitted, and yellow spheres highlight the small tetrahedral pores for clarity.

MOF-808 materials, designated as MOF-808-PAs (PA = polyamine-substituted anion), involving the covalent incorporation of four different liquid polyamines via two-step functionalization. Combined with four optimized or newly synthesized MOF-808-AA materials, the composition, porosity, and inherent pore characteristics of these compounds have been fully characterized. We found that the CO<sub>2</sub> uptake capacities of these new MOF materials at least double the previously reported uptakes for MOF-808 compounds at DAC conditions.<sup>28</sup> Furthermore, their adsorption and desorption behaviors, overall cycling proficiency, and sorption mechanism have also been evaluated.

## RESULTS AND DISCUSSION

**Design and Synthesis.** Due to its remarkable robustness,<sup>30–32</sup> efficient large-scale preparatory process,<sup>33</sup> and capacity for postsynthetic modifications,<sup>34–37</sup> MOF-808 [Zr<sub>6</sub>O<sub>4</sub>(OH)<sub>4</sub>(BTC)<sub>2</sub>(HCOO)<sub>6</sub>, BTC = 1,3,5-benzenetricarboxylate] (Figure 1a) was chosen as the foundational material for amine functionalization and was synthesized following previously established procedures.<sup>28</sup> Subsequently, MOF-808-FR [Zr<sub>6</sub>O<sub>4</sub>(OH)<sub>10</sub>(BTC)<sub>2</sub>(H<sub>2</sub>O)<sub>6</sub>] was derived through the elimination of formate ligands via hydrochloric acid (HCl) treatment at 85 °C for a duration of 5 days. The formate ligands can be nearly entirely removed, as confirmed by digest NMR (Figure S2), and substituted with hydroxide ions or water to achieve a charge balance. The targeted functionalities were then introduced onto the MOF-808 backbones through coordination between Zr(IV) and carboxylate groups, thereby fine-tuning the pore environment and creating specific chemisorption sites tailored for CO<sub>2</sub> capture.

For the preparation of MOF-808-AA sorbents [Zr<sub>6</sub>O<sub>4</sub>(OH)<sub>4</sub>(BTC)<sub>2</sub>(AA)<sub>N</sub>(OH)<sub>6–N</sub>(H<sub>2</sub>O)<sub>6–N</sub>, AA = amino acid anion] (Figure 1b), where *N* denotes the molar equivalence of amino acids per Zr<sub>6</sub>O<sub>4</sub>(OH)<sub>4</sub> cluster (or secondary building unit, SBU), termed as MOF-808-Gly, MOF-808-Pro, MOF-808-Lys, and MOF-808-Arg, four amino acids (Figure 1c), namely, glycine, DL-proline, L-lysine, and L-arginine, were selected with their high pK<sub>a</sub> of the amines<sup>38</sup> to provide strong chemical interaction with CO<sub>2</sub>. The MOF-808-FR powder was immersed in saturated solutions of these amino acids for a duration of 1 to 3 days at the designated temperature. The resultant solid was then collected and subjected to washing with deionized water and acetone, followed by treatment with a 10% solution of 1,8-diazabicyclo[5.4.0]undec-7-ene (DBU) in tetrahydrofuran (THF) to achieve amine deprotonation and hydrochloride salt removal. Further activation was performed by using dynamic vacuum conditions, resulting in the creation of MOF-808-AA samples. In pursuit of enhancing the loading capacity of amino acids and achieving a greater density of chemisorption sites, an extensive screening process has been conducted to assess the optimal loading solvent, temperature, and reaction duration within the synthetic procedure. In order to prevent the potential degradation of MOF-808 during the loading procedure at elevated temperatures caused by the strong basic nature of L-lysine and L-arginine, their hydrochloride salt forms were employed. Moreover, it was determined that ethylene glycol exhibited remarkable solubility and superior loading capabilities for these two amino acid species. This significant finding contributed to a substantial

enhancement in loading efficiency, effectively reducing both the reaction time and solvent usage.

On the other hand, a two-step polyamine functionalization strategy has been devised to develop a new series of functionalized MOF-808. Initially, 3-chloropropionic acid was introduced by binding its carboxylate groups to the Zr(IV) of MOF-808 coordinatively. Parallel to the synthetic procedure implemented for the MOF-808-AA series, the process began by immersing the MOF-808-FR powder in a saturated aqueous solution of 3-chloropropionic acid at 85 °C with the solution being freshly replenished within a 3-day interval. After the solvent exchange and activation process, it yielded MOF-808-EtCl  $[\text{Zr}_6\text{O}_4(\text{OH})_4(\text{BTC})_2(\text{EtCl})_{3.21}(\text{OH})_{2.79}(\text{H}_2\text{O})_{2.79}]$ , with EtCl = 3-chloropropionic acid anion], serving as the foundation for the following step. Subsequently, the newly synthesized product was treated with the polyamine solutions at 85 °C for 24 h. Four distinct polyamines (Figure 1c), ethylenediamine (EDA), 1,3-diaminopropane (DAP), tris(3-aminoethyl)amine (TAEA), and tris(3-aminopropyl)amine (TAPA), were utilized for this amine functionalization. The covalent incorporation of selected polyamines was executed through nucleophilic substitution, replacing chloride ions of installed 3-chloropropionic acid. The resulting solid was then collected, subjected to washing, and activated, ultimately yielding MOF-808-PA with a general empirical formula of  $[\text{Zr}_6\text{O}_4(\text{OH})_4(\text{BTC})_2(\text{PA})_N(\text{EtCl})_{3.21-N}(\text{OH})_{2.79}(\text{H}_2\text{O})_{2.79}]$ , with PA = polyamine-substituted EtCl anion] (Figure 1b), where *N* denotes the molar equivalence of substituted polyamines per SBU, termed as MOF-808-EDA, MOF-808-DAP, MOF-808-TAEA, and MOF-808-TAPA. This strategic approach notably enhanced the density of accessible sorption sites, with a particularly pronounced effect observed with TAEA and TAPA, effectively doubling the count of primary amine groups per loaded molecule (Table S3), ultimately contributing to enhanced CO<sub>2</sub> uptake capabilities.

The composition of the functionalized MOF-808 samples was comprehensively determined through an array of analytical techniques, encompassing liquid-state <sup>1</sup>H nuclear magnetic resonance (NMR) measurements, potentiometric acid–base titration, and scanning electron microscopy (SEM) with energy-dispersive X-ray spectroscopy (EDS). To further characterize the samples, nitrogen sorption isotherm and powder X-ray diffraction (PXRD) analyses were employed to investigate their porosity and crystallinity. Additionally, water vapor isotherm measurements were conducted to explore the influence of water on CO<sub>2</sub> capture. To delve into the CO<sub>2</sub> uptake performance under distinct conditions, both the CO<sub>2</sub> sorption isotherm and dynamic breakthrough measurements were undertaken. These investigations aimed to shed light on the samples' performance at DAC conditions, in dry environments or in the presence of water. Furthermore, the desorption behavior and cycling performance were evaluated to gauge the efficiency and stability of the functionalized MOF-808 materials. Finally, solid-state NMR and temperature-programmed desorption measurements were employed to decipher the chemisorption mechanism between amine functional groups and CO<sub>2</sub> with or without the presence of water.

**Structural and Compositional Characterization.** The retention of crystallinity across all modified MOF-808 variants was evident in the PXRD measurements (Section S5). In comparison with the simulated PXRD pattern of MOF-808, there have been no noticeable phase changes or degradation

observed in the MOF-808-AA series following the post-synthetic functionalization process. For the MOF-808-PA series, some minor degradation was observed, which was likely linked to the disorder introduced by the incorporation of polyamine molecules into the MOF structure. This outcome underscored the resilience of MOF-808, solidifying its potential as a robust platform for targeted applications through postsynthetic modification.

To assess the loading quantity of the designated molecules, we fully hydrolyzed the activated functionalized MOF samples with the aid of hydrofluoric acid (HF) and deuterium chloride (DCl) within a solvent mixture of DMSO-*d*<sub>6</sub> and deuterium oxide (D<sub>2</sub>O). The identification of the loaded molecules was achieved through the introduction of minute quantities of pure molecules into the MOF samples, which were subsequently subjected to analysis via digest NMR (Section S3). The distinct peaks attributable to the targeted molecules within the resulting spectra were discernible through an increased integration. Upon this analytical framework, the loading numbers of amino acids per secondary building unit (SBU) of MOF-808-Gly and MOF-808-Pro were quantified as 4.90 and 3.19 (Figures S3 and S4), respectively. These values translated to loaded quantities of 3.28 and 2.05 mmol g<sup>-1</sup> (Figure 2). For MOF-808-Lys and MOF-808-Arg, the

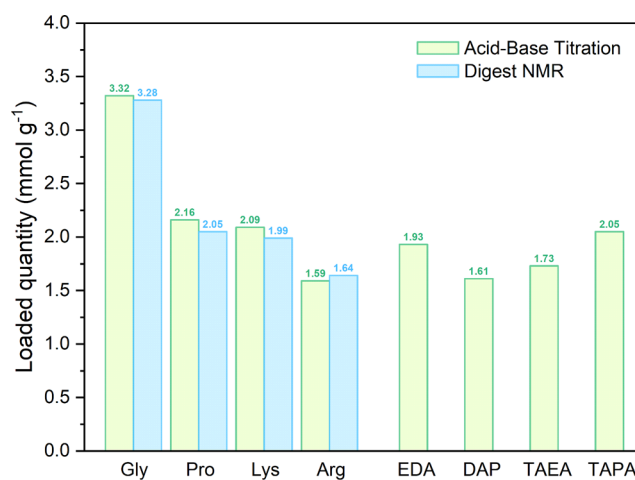


**Figure 2.** Comparison of loaded amino acids/polyamines in the MOF-808-AA and MOF-808-PA series by employing acid–base titration (light green) and <sup>1</sup>H digest NMR (light blue).

established loading numbers were 2.81 and 2.77 per SBU (Figures S5 and S6), which correspond to the loaded quantities of 1.99 and 1.64 mmol g<sup>-1</sup>. Nevertheless, featuring two primary amines per molecule, both MOF-808-Lys and MOF-808-Arg possess a double quantity in effective amine content, measuring at 3.98 and 3.28 mmol g<sup>-1</sup>, respectively. As a result, MOF-808-Lys emerged as the exemplar within the series, boasting the highest effective amine loading.

On the contrary, quantifying the loaded polyamine content using digest NMR presents a considerable challenge due to changes in chemical shifts following covalent incorporation. Thus, the utilization of potentiometric acid–base titration<sup>39</sup> (Section S4) served as a viable alternative to evaluate the amount of basic components within the MOF-808-PA series—specifically, the amine functionalities, which also allowed for the assessment of the quantity and accessibility of functionalized polyamines. In this method, the MOF samples were

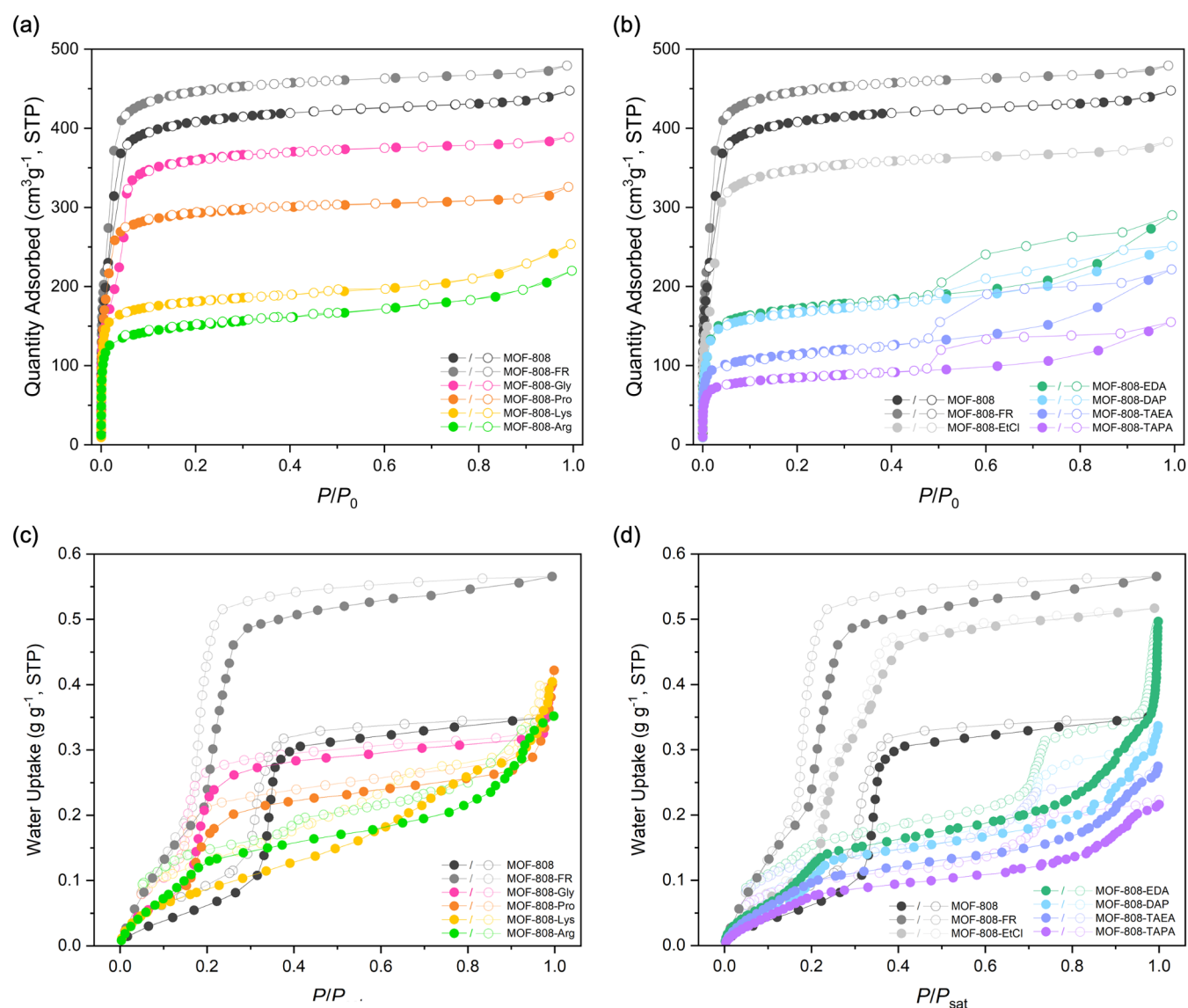


**Figure 3.** Comparison of (a, b)  $N_2$  sorption isotherms at 77 K and (c, d) water sorption isotherms at 25 °C of MOF-808, MOF-808-FR, MOF-808-EtCl, MOF-808-AAs, and MOF-808-PAs. The transparency of the water desorption curves was adjusted for clarity.

ground and suspended in an aqueous  $NaNO_3$  solution. The pH of the solution was adjusted to a range of 10–11 using a 0.1 M aqueous NaOH solution prior to the titration process, which was carried out by adding 0.1 M aqueous HCl solution incrementally. It is worth noting that two distinct equivalence points were manifested across the titration curves for all MOF-808-PA samples. These points signified the presence of unreacted primary amines and secondary amines, each possessing a different level of basicity. The  $pK_a$  values were calculated accordingly at 9.4–9.8 and 10.2–10.3 for two equivalent points (Table S1), respectively, and the loaded polyamines were also quantified in a range of 1.61–2.05 mmol  $g^{-1}$  of MOF-808-PA series (Figures S12–S15, Table S3). The TAPA variant demonstrated the highest conversion rate (98.1%) based on the loading of 3-chloropropionic acid with a value of 2.09 mmol  $g^{-1}$  using digestion NMR (Figure S7), and this was accompanied by the highest gravimetric primary amine loading, reaching 4.10 mmol  $g^{-1}$ . Additionally, the potentiometric acid–base titration method was also employed to ascertain the loading of amino acids within the MOF-808-AA series (Figures S8–S11, Table S2). For MOF-808-Lys and

MOF-808-Arg, two equivalence points can be observed, indicating the number of basic functionality. Remarkably, the results obtained from this titration process aligned closely with values acquired through digestion NMR (Figure 2). The great agreement exhibited the reliability of the analytical procedure, furnishing an invaluable strategy for the evaluation of active sites for use in  $CO_2$  capture applications.

The effectiveness of the two-step postsynthetic functionalization process for the MOF-808-PA series was validated through SEM–EDS measurements (Section S6). In the pristine MOF-808 sample, no signals associated with Cl or N were detected. Upon introduction of 3-chloropropionic acid, the MOF-808-EtCl sample exhibited a noticeable Cl signal, confirming the successful molecule installation. Following the subsequent polyamine functionalization step, a reduction in the Cl signal intensity was observed, accompanied by an increase in the N signal intensity. These observations pointed to the elimination of Cl atoms via nucleophilic substitution and the incorporation of polyamines. This analysis thus reinforced the positive results of the successful functionalization process within the MOF-808-PA series.

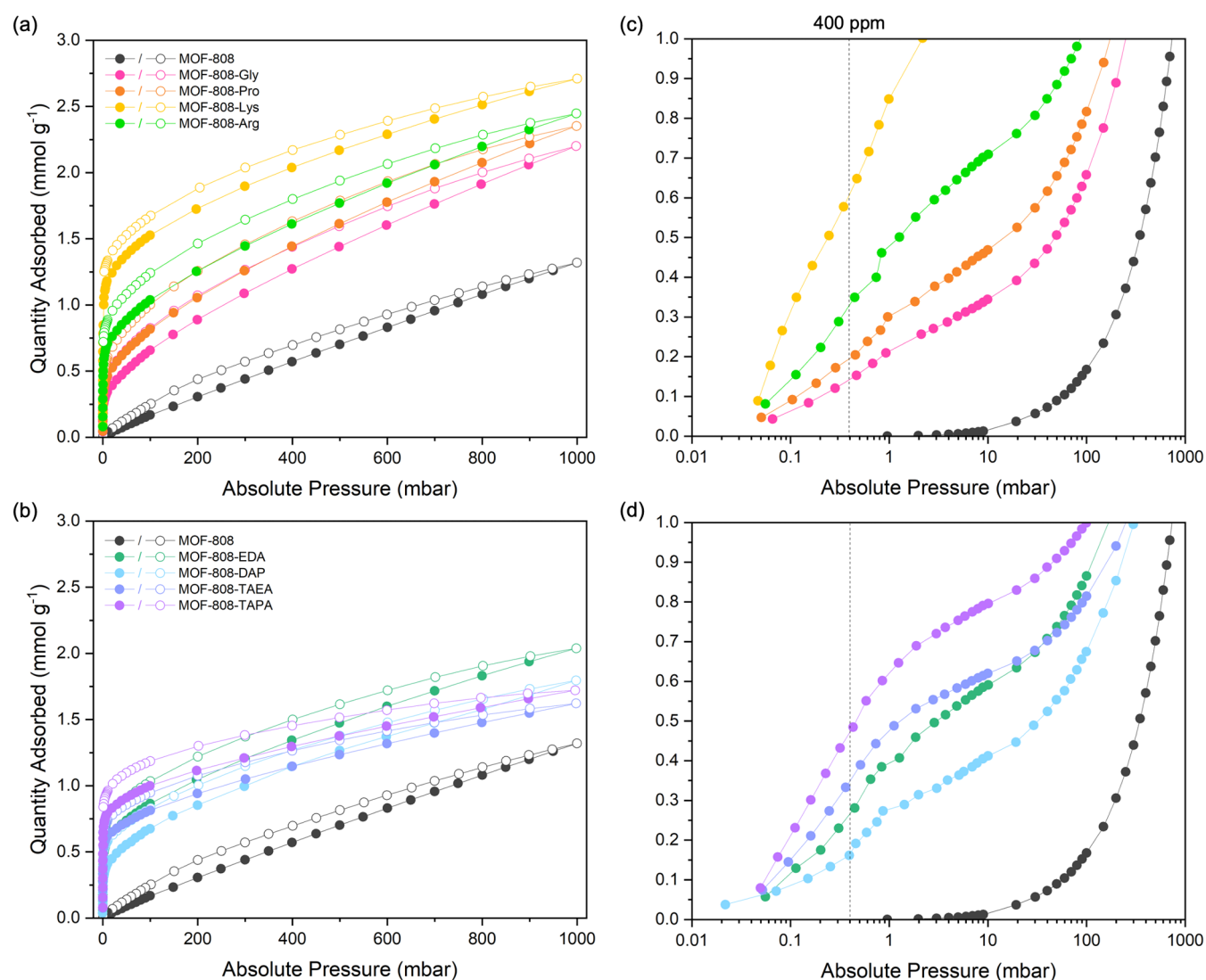


**Figure 4.** Comparison of CO<sub>2</sub> sorption isotherms measured at 25 °C for (a) MOF-808 and the MOF-808-AA series and (b) MOF-808 and the MOF-808-PA series with pressure plotted on a linear scale and a logarithmic scale (c, d) to highlight the uptake at the DAC-relevant pressure.

**Nitrogen and Water Sorption Isotherms.** Nitrogen sorption isotherms were measured at a temperature of 77 K to investigate the permanent porosity and pore size distribution of different variants of MOF-808 (Figure 3 and Section S7). The comparison between MOF-808 and MOF-808-FR showed that the nitrogen uptake increased after the removal of formate ligands, associated with a slight increase in the calculated Brunauer–Emmett–Teller (BET) surface area from 1545 to 1610 m<sup>2</sup> g<sup>-1</sup>. This phenomenon can be explained by the elimination of formate ligands, which resulted in a larger effective volume. In contrast, when examining the MOF-808-AA series, the introduction of amino acids led to a decrease in nitrogen sorption capacities, resulting in both lower BET surface areas (ranging from 573 to 1361 m<sup>2</sup> g<sup>-1</sup>) and pore sizes (ranging from 8.5 to 14.9 Å). This decrease was attributed to factors such as the loading number and the molecular size of the amino acids. In the case of the MOF-808-PA series, the nitrogen sorption capacities also decreased following the incorporation of polyamines and can be translated into BET surface areas ranging from 321 to 676 m<sup>2</sup> g<sup>-1</sup>. One significant observation was the presence of a typical type H3 hysteresis loop<sup>40</sup> during the desorption process for all four samples,

which occurred in the pressure range between  $P/P_0 = 0.5$  and 1.0, usually found on the material with wide pore size distributions. This observation was further supported by the calculated specific pore volumes and pore sizes, which exhibited two distinct values, pointing to the uneven distribution of polyamine incorporation. Particularly, the pore size of MOF-808-EtCl closely resembled that of the larger pores within the MOF-808-PA series, indicative of the distribution of unreacted 3-chloropropionic acid. Conversely, the smaller pores represented the areas of concentrated amine functionalities.

To explore the effects of postsynthetically incorporated functionalities on the pore environment, water sorption isotherms were conducted at 298 K (Figure 3, Section S8). In the case of MOF-808, a distinct steep pore-filling step occurred at approximately 35% relative humidity (RH), accompanied by an adsorption capacity of 0.3 g g<sup>-1</sup>. Following the removal of formate groups, water adsorption commenced at lower RH levels and demonstrated a significantly increased total adsorption capacity of 0.55 g g<sup>-1</sup>. This enhancement was attributed to the direct interaction between water molecules and the hydrophilic zirconium nodes within the structure. The

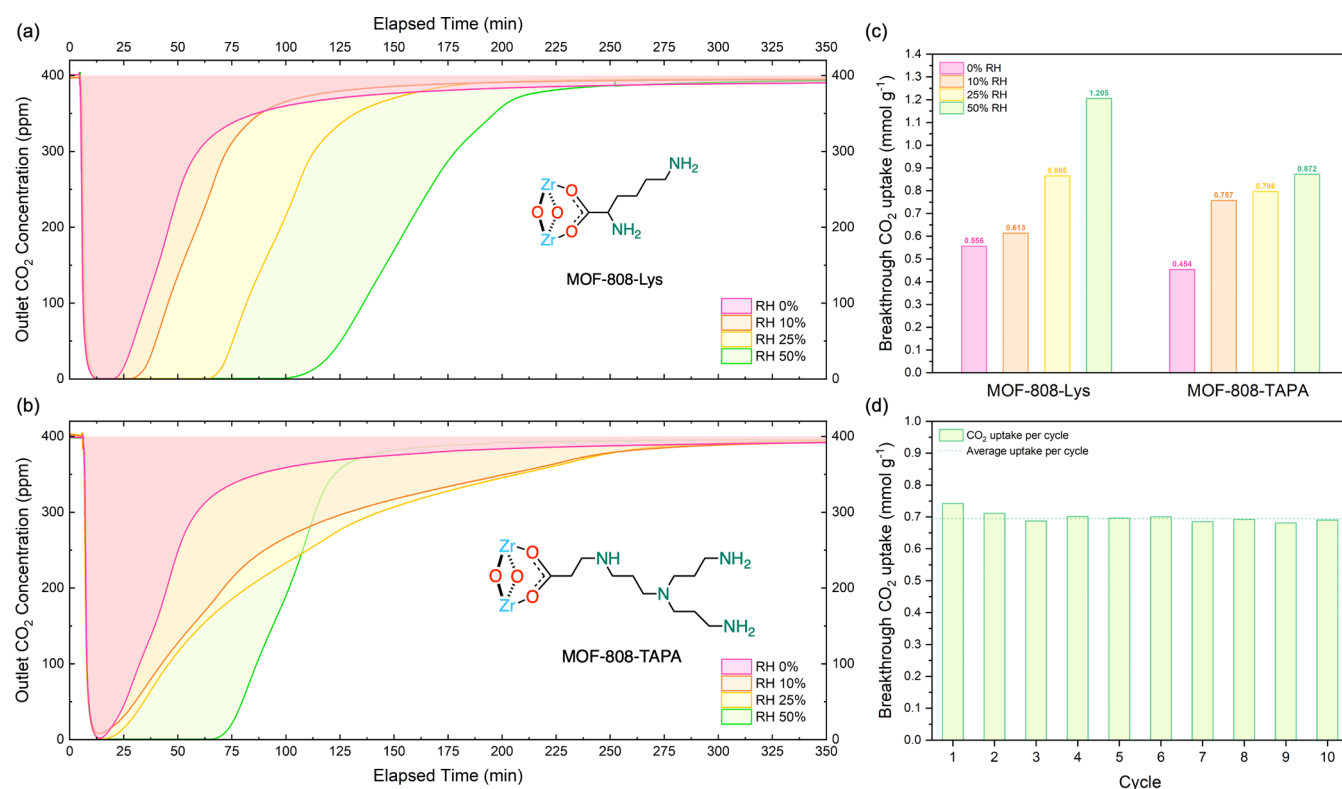


**Figure 5.** Dynamic breakthrough measurements at 25 °C with 0, 10, 25, and 50% RH for (a) MOF-808-Lys and (b) MOF-808-TAPA. In the plot of the outlet CO<sub>2</sub> concentration, the CO<sub>2</sub> uptake can be derived through numerical integration of the marked area. (c) Comparison of CO<sub>2</sub> uptakes of MOF-808-Lys and MOF-808-TAPA by dynamic breakthrough measurements. (d) CO<sub>2</sub> uptakes of MOF-808-Lys at 400 ppm, 50% RH derived from the temperature-swing cycling measurement. The average working capacity was 0.696 mmol g<sup>-1</sup> cycle<sup>-1</sup>.

introduction of amino acids into the MOF-808-AA series similarly resulted in an early onset of water sorption at lower RH levels. However, the overall uptake capacity diminished notably when compared to the original MOF-808. Within the MOF-808-PA series, a hysteresis phenomenon was also observed in the water sorption behavior. In summary, all variants of MOF-808 exhibited great affinity for water molecules, indicating a conducive environment for robust interactions with CO<sub>2</sub>.

**Carbon Dioxide Sorption Analysis.** To evaluate the CO<sub>2</sub> adsorption capacity at a concentration of 400 ppm, which approximates atmospheric CO<sub>2</sub> levels, dry CO<sub>2</sub> sorption isotherms were measured for all variants of MOF-808 as well as the pristine MOF-808 at 298 K (Figure 4a, Section S9). Despite having the highest BET surface area among all of the candidates, MOF-808 exhibited the lowest CO<sub>2</sub> uptake across the entire pressure range from 0 to 1000 mbar, which suggests a lack of strong adsorption sites for CO<sub>2</sub> molecules within MOF-808. In contrast, all amine-functionalized MOF-808 variants displayed significantly enhanced CO<sub>2</sub> uptakes, even though they featured lower porosity compared to the pristine framework. Within the MOF-808-AA series (Figure 4a), namely, MOF-808-Gly, MOF-808-Pro, and MOF-808-Arg, they demonstrated the ability to adsorb CO<sub>2</sub> within the range of 0.142–0.342 mmol g<sup>-1</sup> at this DAC-relevant CO<sub>2</sub> concentration. Particularly noteworthy is MOF-808-Lys, which displayed an uptake of 0.612 mmol g<sup>-1</sup>, which is the highest among all functionalized MOF-808 sorbents. This increased level of CO<sub>2</sub> adsorption can be credited to the highly reactive amine groups within the pores, providing strong chemisorption sites for CO<sub>2</sub> molecules. Furthermore, the

quantity of CO<sub>2</sub> captured was influenced by a combination of factors including the effective gravimetric loading, basicity, and accessibility of these amine species. In the cases of MOF-808-Lys and MOF-808-Arg, their high pK<sub>a</sub> values and substantial gravimetric loading of amines created environments with more reactive and densely packed sorption sites for CO<sub>2</sub>, resulting in higher uptake compared to those of MOF-808-Gly and MOF-808-Pro. The disparity in uptake between MOF-808-Lys and MOF-808-Arg can be attributed to the lower pore accessibility of the latter, which was due to greater steric hindrance resulting from the larger molecular size of L-arginine and the incomplete removal of residual ethylene glycol (Figure S6). In summary, among the studied variants, MOF-808-Lys demonstrated the highest CO<sub>2</sub> uptake, showcasing its superior performance in this regard.

In the MOF-808-PA series (Figure 4b), the CO<sub>2</sub> uptakes at 400 ppm ranged from 0.175 to 0.498 mmol g<sup>-1</sup>, also exhibiting a significant increase in CO<sub>2</sub> uptake compared to pristine MOF-808 due to the two-step polyamine installation. MOF-808-TAPA stood out with the highest gravimetric amine loading, consequently yielding the highest CO<sub>2</sub> capture performance. Furthermore, despite both being functionalized with diamine species, MOF-808-EDA presented a slightly higher CO<sub>2</sub> uptake than that of MOF-808-DAP, which suggested that the amount of CO<sub>2</sub> adsorbed is influenced not only by basicity but also by the quantity of amine loading. It is important to highlight that the CO<sub>2</sub> sorption performance of the MOF-808-PA series differed notably from that of the MOF-808-AA series at high-pressure ranges of CO<sub>2</sub>. Typically, the variants in the MOF-808-AA series exhibited higher uptakes in the high-pressure range compared with the MOF-

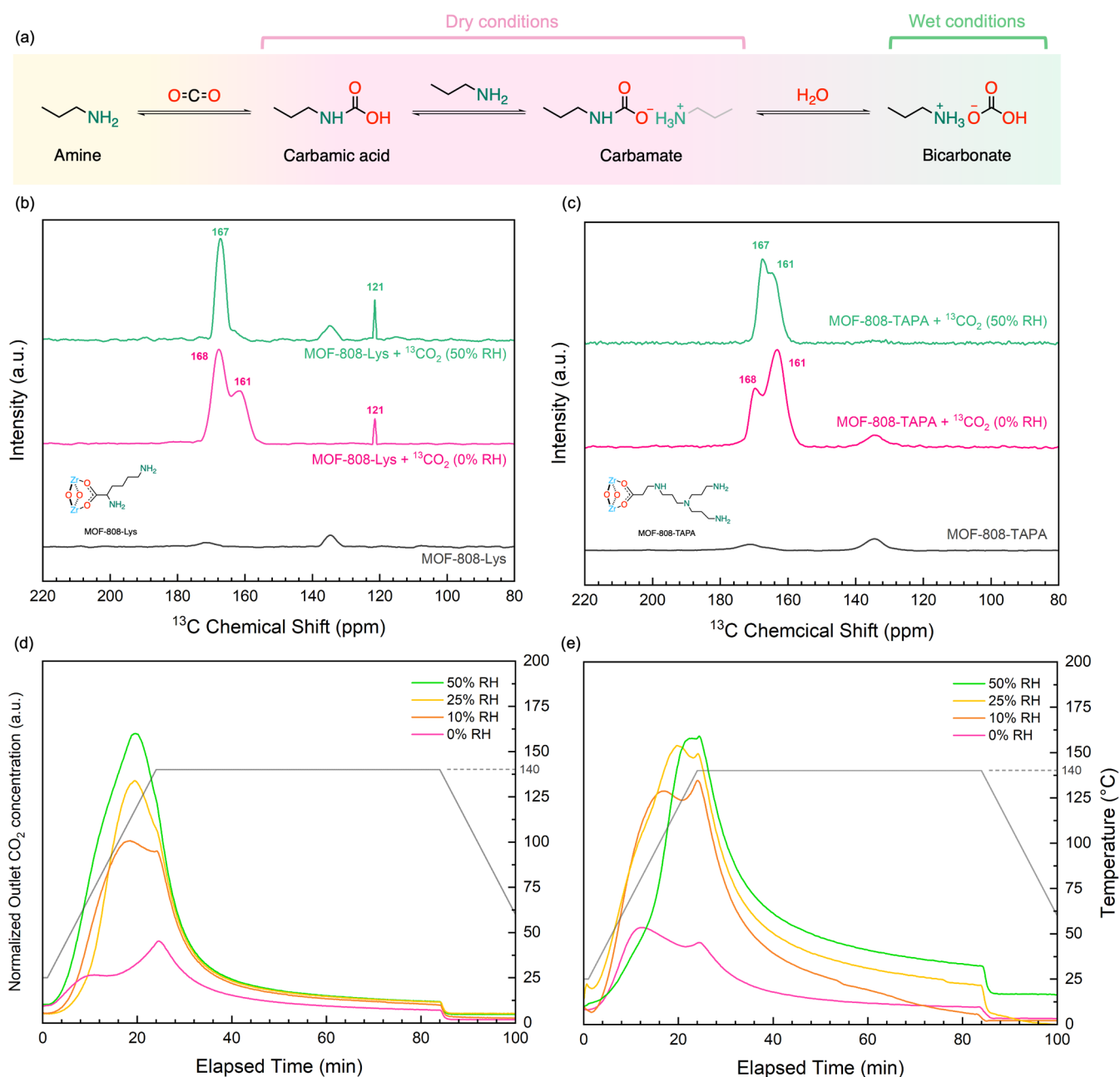


**Figure 6.** (a) Chemisorption mechanism of amines and CO<sub>2</sub> in dry conditions and in the presence of water. (b, c) <sup>13</sup>C solid-state NMR spectra on MOF-808-Lys and MOF-808-TAPA. Bottom: pristine MOF samples; middle: <sup>13</sup>CO<sub>2</sub> dosing under dry conditions; top: <sup>13</sup>CO<sub>2</sub> dosing with 50% RH. (d, e) Temperature-programmed desorption measurements of MOF-808-Lys and MOF-808-TAPA with different RHs.

808-PA series. This phenomenon was likely attributed to the generally lower BET surface area of the MOF-808-PA samples, resulting in reduced physisorption of CO<sub>2</sub>. The CO<sub>2</sub> isotherm measurements demonstrated that MOF-808 serves as a robust platform for basic amine functionalization, offering promising chemisorption sites for strong CO<sub>2</sub> interaction, even at relatively low CO<sub>2</sub> partial pressures, which is advantageous for DAC applications.

**Dynamic Breakthrough Measurements.** To further assess the CO<sub>2</sub> capture performance in the context of practical DAC applications, dynamic breakthrough measurements were conducted (Figure 5, Section S10), which is essential since most capturing scenarios involve high gas flow rates and the presence of water. MOF-808-Lys and MOF-808-TAPA were chosen to measure CO<sub>2</sub> uptake under varying RH levels from 0

to 50% to investigate the impact of water vapor. The samples were activated within the reaction column, and the desired gas feed, containing 400 ppm of CO<sub>2</sub> at different humidity levels, was precisely controlled by adjusting the blend ratio of humidified and dry compressed air. The CO<sub>2</sub> uptakes were calculated through numerical integration of the monitored outlet concentrations of CO<sub>2</sub>.

With breakthrough measurement, MOF-808-Lys (Figure 5a) showed a CO<sub>2</sub> uptake of 0.556 mmol g<sup>-1</sup> at dry condition, which represented a 9% decrease when compared to its single-component CO<sub>2</sub> isotherm. The observed decline can be attributed to the limited contact time between the sorbate and the sorbent materials coupled with the sluggish kinetics of the interaction between MOF-808 and CO<sub>2</sub>, which was also noticeable during isotherm measurements. By introducing 10%

RH, the adsorption capacity can be increased to 0.613 mmol g<sup>-1</sup>. Furthermore, the uptake increased to 0.865 mmol g<sup>-1</sup> in the presence of 25% RH as a 56% enhancement compared to its dry breakthrough uptake. Notably, by doubling the RH to 50%, an exceptional boost in CO<sub>2</sub> uptake to 1.205 mmol g<sup>-1</sup> was observed, representing a remarkable 2.17-fold increase over the dry breakthrough uptake and a 1.97-fold increase over the single-component isotherm. This experiment effectively demonstrated that under varying humidity conditions, moisture can significantly enhance the adsorption efficiency of CO<sub>2</sub> to varying degrees. In the case of MOF-808-TAPA (Figure 5b), the CO<sub>2</sub> uptake reached 0.454 mmol g<sup>-1</sup> under dry conditions, which similarly indicates a 9% deviation from the uptake observed in the dry isotherm. The CO<sub>2</sub> uptake increased to 0.757 mmol g<sup>-1</sup> in the presence of 10% RH, translating to a 67% enhancement. Elevating the humidity to 25% did not yield a significant increase, resulting in an uptake of only 0.796 mmol g<sup>-1</sup>. Finally, employing a 50% RH condition allowed for an uptake of 0.872 mmol g<sup>-1</sup>, marking a 75% increase in comparison to the uptake observed in the dry isotherm. Interestingly, the breakthrough sorption behavior of MOF-808-TAPA differed from that of MOF-808-Lys, as the increase in outlet CO<sub>2</sub> concentration was much slower in the presence of 10 and 25% RH. However, the rate at which the outlet CO<sub>2</sub> concentration increased as adsorption approached saturation largely accelerated with 50% RH, suggesting that water enhances the kinetics of CO<sub>2</sub> uptake of MOF-808-TAPA at high humidity conditions.

Given the remarkable CO<sub>2</sub> uptake in humid conditions, a temperature-swing cycling test (Figure 5c, Section S11) was conducted on MOF-808-Lys at DAC condition (400 ppm of CO<sub>2</sub> with 50% RH). For the measurement efficiency, a quick scan process was employed: both the sorption measurement and the regeneration process were set to conclude when the outlet CO<sub>2</sub> concentration reached 380 and 20 ppm, respectively. While this approach resulted in some partial CO<sub>2</sub> uptake loss, it still allowed for the evaluation of the reproducibility of the sorption–desorption behavior. The measured uptake capacity was determined to be 0.696 mmol g<sup>-1</sup> cycle<sup>-1</sup> over 10 consecutive cycles without significant decay. Nitrogen sorption isotherm measurements and PXRD analysis were performed on MOF-808-Lys after the 10-cycle breakthrough measurement to assess the sorbent's durability (Section S11). No substantial changes in either characterization were observed, indicating retention of the material.

**Sorption Mechanism Study.** To examine the sorption characteristics of amine-functionalized MOF-808, solid-state cross-polarization magic-angle spinning (CP-MAS) <sup>13</sup>C NMR spectra were measured for MOF-808-Lys, and MOF-808-TAPA (Figure 6b,c). This analysis aimed to assess alterations in the chemical composition before and after the introduction of <sup>13</sup>CO<sub>2</sub>, in the presence and absence of water. Hence, the solid-state NMR spectra of these samples were measured under three distinct conditions: (1) activated samples, (2) adsorption of CO<sub>2</sub> under dry condition, and (3) adsorption of CO<sub>2</sub> with 50% RH.

In the <sup>13</sup>C NMR spectra, weak signals at 172 and 134 ppm were observed in both the MOF variants before and after CO<sub>2</sub> sorption, which correspond to the carboxylate and aromatic carbons of the MOF linkers. Both MOF variants were exposed to <sup>13</sup>CO<sub>2</sub> under dry conditions and at 50% RH at 298 K for 24 h. In both samples, two distinct signals at 161 and 168 ppm appeared after loading <sup>13</sup>CO<sub>2</sub> under dry conditions, indicating

the formation of carbamic acid or carbamate<sup>28,29</sup> through covalent interaction between <sup>13</sup>CO<sub>2</sub> and primary amine moieties. For the wet conditions, notably, MOF-808-Lys exhibited a single signal at 167 ppm under 50% RH (Figure 6b), attributed to ammonium bicarbonate formation.<sup>28,29</sup> The presence of water enhanced the amine utilization efficiency through the formation of bicarbonate species, resulting in increased CO<sub>2</sub> uptake compared to the dry conditions. Conversely, MOF-808-TAPA presented two signals under humid conditions (Figure 6c), possibly due to incomplete conversion from carbamic acid/carbamate to bicarbonate. This discrepancy in conversion may be linked to the higher water uptake by MOF-808-Lys (~0.17 g g<sup>-1</sup>) compared to that by MOF-808-TAPA (~0.09 g g<sup>-1</sup>) at 50% RH. The incomplete conversion of bicarbonate in MOF-808-TAPA led to a lower increase in CO<sub>2</sub> uptake by water vapor compared to that by MOF-808-Lys during the dynamic breakthrough measurement. Furthermore, a signal at 121 ppm was observed in the MOF-808-Lys sample, both with and without the presence of water. This signal was ascribed to physisorbed <sup>13</sup>CO<sub>2</sub>. In contrast, free <sup>13</sup>CO<sub>2</sub> was not detected in the MOF-808-TAPA sample. Due to the presence of functionalized branched amines, the BET surface area of MOF-808-TAPA (321 m<sup>2</sup> g<sup>-1</sup>) was lower than half that of MOF-808-Lys (701 m<sup>2</sup> g<sup>-1</sup>), which made it challenging for MOF-808-TAPA to accommodate more CO<sub>2</sub> molecules within its pores. This phenomenon provided an explanation for the observed lower CO<sub>2</sub> uptakes in the high-pressure ranges of the MOF-808-PA series when compared to the MOF-808-AA series in the context of single-component CO<sub>2</sub> isotherms.

Temperature-programmed desorption measurement (Figure 6d,e) was employed to investigate the adsorption–desorption behavior of the selected materials. Utilizing a highly sensitive mass spectrometer detector allowed for the differentiation of various species based on their binding affinities with CO<sub>2</sub>. Prior to the measurement, the MOF powder was saturated with CO<sub>2</sub> at different RH. The temperature was then ramped from 25 to 140 °C with the heat ramp at 5 °C min<sup>-1</sup> and held for 60 min. For MOF-808-Lys, two desorption peaks at 70 and 140 °C were observed at 0% RH, indicating the presence of two species with distinct binding affinities interacting with CO<sub>2</sub>, corresponding to the carbamic acid and carbamate pair. As the humidity increased, these two peaks gradually disappeared, and a new peak emerged at 120 °C, signifying the desorption of CO<sub>2</sub> from the bicarbonate. MOF-808-TAPA exhibited similar results under dry conditions. Conversely, the desorption peak at 140 °C persisted even under high RH as 50%, suggesting an incomplete conversion from carbamic acid/carbamate to bicarbonate. These observations aligned well with the findings in solid-state NMR, providing valuable insights into the sorption mechanism study.

## CONCLUSIONS

We employed two distinct amine functionalization strategies for MOF-808, utilizing amino acids that are directly bound to the zirconium SBU, and polyamine incorporation via two-step nucleophilic substitution. The resulting compounds demonstrated exceptional CO<sub>2</sub> capture capacity and stability when exposed to ambient air containing water vapor. The quantity of loaded amine species, the sorption behavior, and the sorption chemistry were fully characterized. This research showcased the extensive tunability of MOF-808 and unveiled substantial

potential for amine functionalization in the development of solid-state sorbents for DAC-relative applications.

## ■ ASSOCIATED CONTENT

### SI Supporting Information

The Supporting Information is available free of charge at <https://pubs.acs.org/doi/10.1021/jacs.3c14125>.

Detailed experimental procedures, synthesis, and characterization details of the reported compounds, including digest NMR, potentiometric acid–base titration, PXRD, SEM–EDS analysis, nitrogen sorption isotherms, water vapor sorption isotherms, CO<sub>2</sub> sorption isotherms, and dynamic breakthrough measurements (PDF)

## ■ AUTHOR INFORMATION

### Corresponding Authors

Jorge A. R. Navarro – *Departamento de Química Inorgánica, Universidad de Granada, Granada 18071, Spain;*  
orcid.org/0000-0002-8359-0397; Email: [jarn@ugr.es](mailto:jarn@ugr.es)

Omar M. Yaghi – *Department of Chemistry and Kavli Energy Nano Sciences Institute, University of California, Berkeley, California 94720, United States; Bakar Institute of Digital Materials for the Planet, College of Computing, Data Science, and Society, University of California, Berkeley, California 94720, United States; KACST-UC Berkeley Center of Excellence for Nanomaterials for Clean Energy Applications, King Abdulaziz City for Science and Technology, Riyadh 11442, Saudi Arabia;* orcid.org/0000-0002-5611-3325; Email: [yaghi@berkeley.edu](mailto:yaghi@berkeley.edu)

### Authors

Oscar Iu-Fan Chen – *Department of Chemistry and Kavli Energy Nano Sciences Institute, University of California, Berkeley, California 94720, United States; Bakar Institute of Digital Materials for the Planet, College of Computing, Data Science, and Society, University of California, Berkeley, California 94720, United States;* orcid.org/0000-0003-4361-0768

Cheng-Hsin Liu – *Department of Chemistry and Kavli Energy Nano Sciences Institute, University of California, Berkeley, California 94720, United States; Bakar Institute of Digital Materials for the Planet, College of Computing, Data Science, and Society, University of California, Berkeley, California 94720, United States;* orcid.org/0009-0000-7140-1061

Kaiyu Wang – *Department of Chemistry and Kavli Energy Nano Sciences Institute, University of California, Berkeley, California 94720, United States; Bakar Institute of Digital Materials for the Planet, College of Computing, Data Science, and Society, University of California, Berkeley, California 94720, United States*

Emilio Borrego-Marin – *Departamento de Química Inorgánica, Universidad de Granada, Granada 18071, Spain*

Haozhe Li – *Department of Chemistry and Kavli Energy Nano Sciences Institute, University of California, Berkeley, California 94720, United States; Bakar Institute of Digital Materials for the Planet, College of Computing, Data Science, and Society, University of California, Berkeley, California 94720, United States*

Ali H. Alawadhi – *Department of Chemistry and Kavli Energy Nano Sciences Institute, University of California, Berkeley, California 94720, United States; Bakar Institute of Digital Materials for the Planet, College of Computing, Data Science,*

*and Society, University of California, Berkeley, California 94720, United States;* orcid.org/0000-0003-2680-5221

Complete contact information is available at: <https://pubs.acs.org/doi/10.1021/jacs.3c14125>

### Notes

The authors declare the following competing financial interest(s): Omar M. Yaghi is co-founder of ATOCO Inc., aiming at commercializing related technologies.

## ■ ACKNOWLEDGMENTS

This work was financially supported by the Department of Energy under Award DE-FE0031956. The authors thank Ephraim Neumann from the Yaghi research group for his help with SEM–EDS measurement. They also thank Zihui Zhou from the Yaghi research group for helpful discussions with material characterizations; Dr. Mark D. Doherty, Dr. David R. Moore, and their colleagues at GE Research for insightful discussions regarding material synthesis and characterizations; and Drs. Hasan Celik, Raynald Giovine, and UC Berkeley's NMR facility in the College of Chemistry (CoC-NMR) for spectroscopic assistance. The instrument used in this work was supported by the National Science Foundation under Grant No. 2018784. J.A.R.N. is grateful to the financial support from Spanish Ministerio de Universidades for a Salvador Madariaga-Fulbright grant (PRX21/00093) and from Ministerio de Ciencia e Innovación Agencia Estatal de Investigación (MCIN/AEI/10.13039/501100011033, Project PID2020-113608RB-I00; TED2021-129886B-C41). O.I.-F.C. acknowledges financial support from the Taiwan Ministry of Education. E.B.-M. acknowledges Plan Propio de Investigación-Universidad de Granada for a predoctoral fellowship.

## ■ REFERENCES

- (1) IPCC 2023. *Summary for Policymakers. In: Climate Change 2023: Synthesis Report. Contribution of Working Groups I, II and III to the Sixth Assessment Report of the Intergovernmental Panel on Climate Change*; IPCC: Geneva, Switzerland, 2023.
- (2) Sanz-Pérez, E. S.; Murdock, C. R.; Didas, S. A.; Jones, C. W. Direct Capture of CO<sub>2</sub> from Ambient Air. *Chem. Rev.* **2016**, *116*, 11840–11876.
- (3) Zhu, X.; Xie, W.; Wu, J.; Miao, Y.; Xiang, C.; Chen, C.; Ge, B.; Gan, Z.; Yang, F.; Zhang, M.; O'Hare, D.; Li, J.; Ge, T.; Wang, R. Recent Advances in Direct Air Capture by Adsorption. *Chem. Soc. Rev.* **2022**, *51*, 6574–6651.
- (4) IEA. Direct Air Capture, 2022. <https://www.iea.org/reports/direct-air-capture-2022>.
- (5) Su, F.; Lu, C.; Kuo, S.-C.; Zeng, W. Adsorption of CO<sub>2</sub> on Amine-Functionalized Y-type Zeolites. *Energy Fuels* **2010**, *24*, 1441–1448.
- (6) Bollini, P.; Didas, S. A.; Jones, C. W. Amine-oxide Hybrid Materials for Acid Gas Separations. *J. Mater. Chem.* **2011**, *21*, 15100–15120.
- (7) Lin, Y.; Kong, C.; Chen, L. Amine-Functionalized Metal–Organic Frameworks: Structure, Synthesis and Applications. *RSC Adv.* **2016**, *6*, 32598–32614.
- (8) Varghese, A. M.; Karanikolos, G. N. CO<sub>2</sub> Capture Adsorbents Functionalized by Amine-Bearing Polymers: A Review. *Int. J. Greenhouse Gas Control* **2020**, *96*, No. 103005.
- (9) Lyu, H.; Li, H.; Hanikel, N.; Wang, K.; Yaghi, O. M. Covalent Organic Frameworks for Carbon Dioxide Capture from Air. *J. Am. Chem. Soc.* **2022**, *144*, 12989–12995.
- (10) Fan, Y.; Jia, X. Progress in Amine-Functionalized Silica for CO<sub>2</sub> Capture: Important Roles of Support and Amine Structure. *Energy Fuels* **2022**, *36*, 1252–1270.

- (11) Sanz, R.; Calleja, G.; Arencibia, A.; Sanz-Pérez, E. S. Development of High Efficiency Adsorbents for CO<sub>2</sub> Capture Based On A Double-Functionalization Method of Grafting and Impregnation. *J. Mater. Chem. A* **2013**, *1*, 1956–1962.
- (12) Rochelle, G. T. Amine Scrubbing for CO<sub>2</sub> Capture. *Science* **2009**, *325*, 1652–1654.
- (13) Kiani, A.; Jiang, K.; Feron, P. Techno-Economic Assessment for CO<sub>2</sub> Capture from Air Using a Conventional Liquid-Based Absorption Process. *Front. Energy Res.* **2020**, *8*, 92.
- (14) Kumar, A.; Madden, D. G.; Lusi, M.; Chen, K. J.; Daniels, E. A.; Curtin, T.; Perry, J. J. t.; Zaworotko, M. J. Direct Air Capture of CO<sub>2</sub> by Physisorbent Materials. *Angew. Chem., Int. Ed.* **2015**, *54*, 14372–14377.
- (15) Lu, W.; Sculley, J. P.; Yuan, D.; Krishna, R.; Zhou, H.-C. Carbon Dioxide Capture from Air Using Amine-Grafted Porous Polymer Networks. *J. Phys. Chem. C* **2013**, *117*, 4057–4061.
- (16) Sujan, A. R.; Pang, S. H.; Zhu, G.; Jones, C. W.; Lively, R. P. Direct CO<sub>2</sub> Capture from Air Using Poly(Ethylenimine)-Loaded Polymer/Silica Fiber Sorbents. *ACS Sustainable Chem. Eng.* **2019**, *7*, 5264–5273.
- (17) Cherevotan, A.; Raj, J.; Peter, S. C. An Overview of Porous Silica Immobilized Amines for Direct Air CO<sub>2</sub> Capture. *J. Mater. Chem. A* **2021**, *9*, 27271–27303.
- (18) Anyanwu, J.-T.; Wang, Y.; Yang, R. T. CO<sub>2</sub> Capture (Including Direct Air Capture) and Natural Gas Desulfurization of Amine-Grafted Hierarchical Bimodal Silica. *Chem. Eng. J.* **2022**, *427*, No. 131561.
- (19) Anyanwu, J.-T.; Wang, Y.; Yang, R. T. Amine-Grafted Silica Gels for CO<sub>2</sub> Capture Including Direct Air Capture. *Ind. Eng. Chem. Res.* **2020**, *59*, 7072–7079.
- (20) Sumida, K.; Rogow, D. L.; Mason, J. A.; McDonald, T. M.; Bloch, E. D.; Herm, Z. R.; Bae, T. H.; Long, J. R. Carbon Dioxide Capture in Metal-Organic Frameworks. *Chem. Rev.* **2012**, *112*, 724–781.
- (21) McDonald, T. M.; Lee, W. R.; Mason, J. A.; Wiers, B. M.; Hong, C. S.; Long, J. R. Capture of Carbon Dioxide From Air and Flue Gas in The Alkylamine-Appended Metal–Organic Framework mmen-Mg<sub>2</sub> (dobpdc). *J. Am. Chem. Soc.* **2012**, *134*, 7056–7065.
- (22) Lee, W. R.; Hwang, S. Y.; Ryu, D. W.; Lim, K. S.; Han, S. S.; Moon, D.; Choi, J.; Hong, C. S. Diamine-Functionalized Metal–Organic Framework: Exceptionally High CO<sub>2</sub> Capacities from Ambient Air and Flue Gas, Ultrafast CO<sub>2</sub> Uptake Rate, and Adsorption Mechanism. *Energy Environ. Sci.* **2014**, *7*, 744–751.
- (23) Shekhah, O.; Belmabkhout, Y.; Chen, Z.; Guillerm, V.; Cairns, A.; Adil, K.; Eddaoudi, M. Made-To-Order Metal-Organic Frameworks for Trace Carbon Dioxide Removal and Air Capture. *Nat. Commun.* **2014**, *5*, No. 4228.
- (24) Bien, C. E.; Chen, K. K.; Chien, S.-C.; Reiner, B. R.; Lin, L.-C.; Wade, C. R.; Ho, W. W. Bioinspired Metal–Organic Framework for Trace CO<sub>2</sub> Capture. *J. Am. Chem. Soc.* **2018**, *140*, 12662–12666.
- (25) Sadiq, M. M.; Batten, M. P.; Mulet, X.; Freeman, C.; Konstas, K.; Mardel, J. I.; Tanner, J.; Ng, D.; Wang, X.; Howard, S.; et al. A Pilot-Scale Demonstration of Mobile Direct Air Capture Using Metal-Organic Frameworks. *Adv. Sustainable Syst.* **2020**, *4*, 2000101.
- (26) Darunte, L. A.; Oetomo, A. D.; Walton, K. S.; Sholl, D. S.; Jones, C. W. Direct Air Capture of CO<sub>2</sub> Using Amine Functionalized MIL-101 (Cr). *ACS Sustainable Chem. Eng.* **2016**, *4*, 5761–5768.
- (27) Zeng, Y.; Zou, R.; Zhao, Y. Covalent Organic Frameworks for CO<sub>2</sub> Capture. *Adv. Mater.* **2016**, *28*, 2855–2873.
- (28) Lyu, H.; Chen, O. I.-F.; Hanikel, N.; Hossain, M. I.; Flaig, R. W.; Pei, X.; Amin, A.; Doherty, M. D.; Impastato, R. K.; Glover, T. G.; Moore, D. R.; Yaghi, O. M. Carbon Dioxide Capture Chemistry of Amino Acid Functionalized Metal–Organic Frameworks in Humid Flue Gas. *J. Am. Chem. Soc.* **2022**, *144*, 2387–2396.
- (29) Flaig, R. W.; Osborn Popp, T. M.; Fracaroli, A. M.; Kapustin, E. A.; Kalmutzki, M. J.; Altamimi, R. M.; Fathieh, F.; Reimer, J. A.; Yaghi, O. M. The Chemistry of CO<sub>2</sub> Capture in An Amine-Functionalized Metal–Organic Framework Under Dry and Humid Conditions. *J. Am. Chem. Soc.* **2017**, *139*, 12125–12128.
- (30) Furukawa, H.; Gándara, F.; Zhang, Y.-B.; Jiang, J.; Queen, W. L.; Hudson, M. R.; Yaghi, O. M. Water Adsorption in Porous Metal–Organic Frameworks and Related Materials. *J. Am. Chem. Soc.* **2014**, *136*, 4369–4381.
- (31) Baek, J.; Rungtaweeworanit, B.; Pei, X.; Park, M.; Fakra, S. C.; Liu, Y.-S.; Matheu, R.; Alshmiri, S. A.; Alshehri, S.; Trickett, C. A.; et al. Bioinspired Metal–Organic Framework Catalysts for Selective Methane Oxidation to Methanol. *J. Am. Chem. Soc.* **2018**, *140*, 18208–18216.
- (32) Hu, Z.; Kundu, T.; Wang, Y.; Sun, Y.; Zeng, K.; Zhao, D. Modulated Hydrothermal Synthesis of Highly Stable MOF-808 (Hf) for Methane Storage. *ACS Sustainable Chem. Eng.* **2020**, *8*, 17042–17053.
- (33) Jiang, J.; Gándara, F.; Zhang, Y.-B.; Na, K.; Yaghi, O. M.; Klemperer, W. G. Superacidity in Sulfated Metal–Organic Framework-808. *J. Am. Chem. Soc.* **2014**, *136*, 12844–12847.
- (34) Mautschke, H.-H.; Drache, F.; Senkovska, I.; Kaskel, S.; i Xamena, F. L. Catalytic Properties of Pristine and Defect-Engineered Zr-MOF-808 Metal Organic Frameworks. *Catal. Sci. Technol.* **2018**, *8*, 3610–3616.
- (35) Zhang, W.; Bu, A.; Ji, Q.; Min, L.; Zhao, S.; Wang, Y.; Chen, J. pK<sub>a</sub>-Directed Incorporation of Phosphonates into MOF-808 via Ligand Exchange: Stability and Adsorption Properties for Uranium. *ACS Appl. Mater. Interfaces* **2019**, *11*, 33931–33940.
- (36) Aunan, E.; Affolter, C. W.; Olsbye, U.; Lillerud, K. P. Modulation of the Thermochemical Stability and Adsorptive Properties of MOF-808 by the Selection of Non-structural Ligands. *Chem. Mater.* **2021**, *33*, 1471–1476.
- (37) Ji, C.; Ren, Y.; Yu, H.; Hua, M.; Lv, L.; Zhang, W. Highly Efficient and Selective Hg (II) Removal from Water by Thiol-Functionalized MOF-808: Kinetic and Mechanism Study. *Chem. Eng. J.* **2022**, *430*, No. 132960.
- (38) Lide, D. R. *CRC Handbook of Chemistry and Physics. A Ready-Reference Book of Chemical and Physical Data*; CRC Press: Boca Raton, FL, 1991.
- (39) Klet, R. C.; Liu, Y.; Wang, T. C.; Hupp, J. T.; Farha, O. K. Evaluation of Brønsted Acidity and Proton Topology in Zr-and Hf-Based Metal–Organic Frameworks Using Potentiometric Acid–Base Titration. *J. Mater. Chem. A* **2016**, *4*, 1479–1485.
- (40) Yurdakal, S.; Garlisi, C.; Özcan, L.; Bellardita, M.; Palmisano, G. (Photo)catalyst Characterization Techniques: Adsorption Isotherms and BET, SEM, FTIR, UV–Vis, Photoluminescence, and Electrochemical Characterizations. In *Heterogeneous Photocatalysis*; Elsevier, 2019.